J. Microbiol. Biotechnol. (2014), 24(4), 453–464
http://dx.doi.org/10.4014/jmb.1310.10095

jmb

# Fabrication of Biogenic Antimicrobial Silver Nanoparticles by *Streptomyces aegyptia* NEAE 102 as Eco-Friendly Nanofactory

**Noura El-Ahmady El-Naggar[1]*, Nayera A. M. Abdelwahed[2], and Osama M. M. Darwesh[3]**

[1]*Department of Bioprocess Development, Genetic Engineering and Biotechnology Research Institute, City of Scientific Research and Technological Applications, Alexandria 21934, Egypt*
[2]*Chemistry of Natural and Microbial Products Department, National Research Center, 12311 Dokki, Cairo, Egypt*
[3]*Agricultural Microbiology Department, Agricultural and Biology Research Division, National Research Center, 12311 Dokki, Cairo, Egypt*

*Received: October 28, 2013*
*Revised: December 22, 2013*
*Accepted: December 24, 2013*

First published online
December 30, 2013

**Corresponding author*
Phone: +(002)01003738444;
Fax: +(002)03-4593423;
E-mail: nouraelahmady@yahoo.com

pISSN 1017-7825, eISSN 1738-8872



The current research was focused on the extracellular biosynthesis of bactericidal silver nanoparticles (AgNPs) using cell-free supernatant of a local isolate previously identified as a novel *Streptomyces aegyptia* NEAE 102. The biosynthesis of silver nanoparticles by *Streptomyces aegyptia* NEAE 102 was quite fast and required far less time than previously published strains. The produced particles showed a single surface plasmon resonance peak at 400 nm by UV–Vis spectroscopy, which confirmed the presence of AgNPs. Response surface methodology was chosen to evaluate the effects of four process variables ($AgNO_3$ concentration, incubation period, pH levels, and inoculum size) on the biosynthesis of silver nanoparticles by *Streptomyces aegyptia* NEAE 102. Statistical analysis of the results showed that the linear and quadratic effects of incubation period, initial pH, and inoculum size had a significant effect ($p < 0.05$) on the biosynthesis of silver nanoparticles by *Streptomyces aegyptia* NEAE 102. The maximum silver nanoparticles biosynthesis (2.5 OD, at 400 nm ) was achieved in runs number 5 and 14 under the conditions of 1 mM $AgNO_3$ (1–1.5% (v/v)), incubation period (72–96 h), initial pH (9–10), and inoculum size (2–4% (v/v)). An overall 4-fold increase in AgNPs biosynthesis was obtained as compared with that of unoptimized conditions. The biosynthesized silver nanoparticles were characterized using UV-VIS spectrophotometer and Fourier transform infrared spectroscopy analysis, in addition to antimicrobial properties. The biosynthesized AgNPs significantly inhibited the growth of medically important pathogenic gram-positive (*Staphylococcus aureus*) and gram-negative bacteria (*Pseudomonas aeruginosa*) and yeast (*Candida albicans*).

**Keywords:** Silver nanoparticles, biosynthesis, antimicrobial activity, *Streptomyces aegyptia* NEAE 102, response surface methodology, energy dispersive X-ray spectroscopy.

## Introduction

Nanomaterials have a long list of applicability in improving human life and its environment. An important area of research in nanotechnology is the biosynthesis of nanoparticles such as nanosilver. The extremely small size and large surface area relative to their volume makes them useful for applications in various fields, such as antibacterials [34], therapeutics [40], high-sensitivity biomolecular detection and diagnostics, silver-nanocoated medical devices [37], optical receptors [26], nonlinear optics, spectrally selective coating for solar energy absorption, biolabeling, intercalation materials for electrical batteries, catalysis in chemical reactions [9], cosmetics, microelectronics, and conductive inks and adhesives [2].

Silver nanoparticles (AgNPs) are currently commonly synthesized by chemical reduction [21], thermal treatment [35], irradiation [30] and laser ablation [38], which are low-yield, energy-intensive, difficult to scale up, often producing high levels of hazardous wastes, and may require the use

of organic solvents and toxic reducing agents like sodium borohydride and N,N-dimethylformamide. Thus, these techniques yield extremely expensive materials. In addition, the produced nanoparticles exhibit undesirable aggregation with time. Hence, a green synthesis method has been developed to obtain biocompatible, cost-effective, clean, nontoxic, easily scaled up for large-scale synthesis, and eco-friendly size-controlled nanoparticles. Microbial properties of bioaccumulation, biosorption, biodetoxification, and biomineralization have been regarded as opportunities to use them as nanofactories for mining nanomaterials [18].

One of the major issues to be considered during synthesis of nanoparticles is their size, depending on which the applications may vary [7]. Biosynthetic methods can be categorized into intracellular and extracellular synthesis according to the place where nanoparticles are formed [36]. For extracellular synthesis, it is reported that a reductase enzyme is released into solution, which reduces a salt to its metallic solid nanoparticles through the catalytic effect [1]. Extracellular secretion of enzymes offers the advantage of obtaining large quantities in a relatively pure state, free from other cellular proteins associated with the organism, and can be easily processed by filtering of the cells and isolating the enzyme for nanoparticles synthesis from cell-free filtrate. Various microorganisms (bacteria, yeast, fungi) are known to synthesize silver nanoparticles. The produced nanoparticles have different sizes and shapes.

The shape of AgNPs, predominantly spherical, is common to microbial-mediated synthesis [31]. Nanoparticles resulting from some microbial processes are composite materials and consist of an inorganic component and a special organic matrix (proteins, lipids, or polysaccharides) and they have unique chemical and physical properties different from the properties of conventionally produced nanoparticles and of other microorganisms even when they are incubated in the same medium under the same conditions [19].

Traditionally, fermentation processes have been optimized by changing one independent variable or factor at a time while keeping the others at some fixed values. The disadvantages of such a classical method are that it is time consuming, laborious, and expensive; in addition, it ignores the combined interactions among different variables employed [6]. Consequently, statistical methods are increasingly preferred for fermentation optimization because they reduce the total number of experiments needed and provide a better understanding of the interactions among factors on the outcome of the fermentation [24]. Response surface methodology (RSM) is a statistical technique based on the fundamental principles of statistics, randomization, replication, and duplication, which simplifies the optimization by studying the mutual interactions among the variables over a range of values in a statistically valid manner. It is an efficient statistical technique for optimization of multiple variables in order to predict the best performance conditions with a minimum number of experiments and explain the individual and interactive effects of test variables on the response [20].

In this study, for the first time, a novel actinomycete strain, *Streptomyces aegyptia* NEAE 102, is utilized for the synthesis of silver nanoparticles.

A statistical approach (central composite design) has been employed in the present study to optimize the extracellular biosynthesis of silver nanoparticles by the novel *Streptomyces aegyptia* NEAE 102. The biosynthesized nanoparticles were characterized for their surface properties using FTIR, in addition to antimicrobial properties using gram-positive, and gram-negative bacterial strains and yeast.

## Materials and Methods

### Microorganisms and Cultural Conditions

The *Streptomyces* sp. used in this study is a local isolate previously identified as the novel *Streptomyces aegyptia* NEAE 102, and its sequencing product was deposited in the GenBank database under Accession No. HQ677021 [5] and was kindly provided by Dr. Noura El-Ahmady El-Naggar (Department of Bioprocess Development, Genetic Engineering and Biotechnology Research Institute, City for Scientific Research and Technologial Applications, Alexandria, Egypt). This isolate was maintained on slopes containing starch-nitrate agar medium of the following composition (g/l): Starch 20; $KNO_3$ 2; $K_2HPO_4$ 1; $MgSO_4{\cdot}7H_2O$ 0.5; NaCl 0.5; $CaCO_3$ 3; $FeSO_4{\cdot}7H_2O$ 0.01; agar 20; and distilled water up to 1 L. Slopes were incubated for a period of 7 days at 30°C. The isolate was stored as spore suspensions in 20% (v/v) glycerol at –20°C for subsequent investigation.

### Inoculum Preparation

Erlenmeyer flasks (250 ml) containing 50 ml of medium consisting of (g/l): Soluble starch 20; $NaNO_3$ 2; $K_2HPO_4$ 1; $MgSO_4{\cdot}7H_2O$ 0.5; and distilled water up to 1 L were inoculated with three disks of 9 mm diameter taken from 7-day-old stock culture grown on starch nitrate agar medium. The flasks were incubated for 48 h in a rotatory incubator shaker at 30ºC and 200 rpm and were used as inoculum for subsequent experiments.

### Extracellular Synthesis of AgNPs

In order to screen an efficient strain for the synthesis of AgNPs, 7 *Streptomyces* strains (*Streptomyces aegyptia* NEAE 102, *Streptomyces viridochromogenes, Streptomyces* sp. NEAE D, *Streptomyces albogriseolus, Streptomyces mutabilis* NEAE F, *Streptomyces* sp. NEAE 126, and

*Streptomyces* sp. NEAE 25) were freshly inoculated in an Erlenmeyer flask containing 50 ml of the production medium consisting of (g/l): Soluble starch 20; $NaNO_3$ 2; $K_2HPO_4$ 1; $MgSO_4 \cdot 7H_2O$ 0.5; and distilled water up to 1 L. The inoculated flasks were incubated on a rotatory incubator shaker at 30°C and 200 rpm for 72 h. After the incubation period, the cell-free supernatant was obtained by centrifugation at 5,000 rpm for 30 min. For the biosynthesis of AgNPs to occur, 1% (v/v) of 1 mM $AgNO_3$ was added to the cell-free supernatant and incubated on an orbital shaker (dark condition) for 24 h at 30°C. The cell-free supernatant without addition of $AgNO_3$ was maintained as a control. Rapid biosynthesis of AgNPs was achieved by addition of silver nitrate solution (1 mM $AgNO_3$) to the cell-free supernatant of *Streptomyces aegyptia* NEAE 102, where immediately it turned to a brown color solution. Consequently, the bioreduction reaction was monitored by visual color change and UV– visible absorbance of the reaction mixture in the 300–600 nm range.

**Experimental Design**

In this study, the effect of four process parameters, namely $AgNO_3$ concentration ($X_1$), incubation period ($X_2$), pH level ($X_3$), and inoculum size ($X_4$), on biosynthesis of silver nanoparticles was studied and optimized using central composite design (CCD). Each factor in the design was studied at five different levels (–2, –1, 0, 1, 2). The coded and actual values of the variables at various levels are given in Table 1. The central values (zero level) chosen for experimental design were 1 mM $AgNO_3$ (1% (v/v)), incubation period 72 h, pH level 8, and inoculum size 4% (v/v). The experimental design used for the study consisted of 30 trials (Table 2). Experiments were conducted in 250 ml Erlenmeyer flasks containing 50 ml of medium prepared according to the design. The flasks were kept in an incubator shaker maintained at 30°C and 200 rpm.

All the experiments were done in duplicate and the average of absorbance at 400 nm, which indicates the biosynthesis of silver nanoparticles obtained, was taken as the dependent variable or response (Y).

The experimental results of CCD were fitted *via* the response surface regression procedure, using the following second-order polynomial equation:

$$Y = \beta_0 + \sum_i \beta_i X_i + \sum_{ii} \beta_{ii} X_i^2 + \sum_{ij} \beta_{ij} X_i X_j \quad (1)$$

where Y is the predicted response, $\beta_0$ is the regression coefficients, $\beta_i$ is the linear coefficient, $\beta_{ii}$ is the quadratic coefficients, $\beta_{ij}$ is the interaction coefficients) and $X_i$ is the coded levels of independent variables. However, in this study, the independent variables were coded as $X_1$, $X_2$, $X_3$, and $X_4$. Thus, the second-order polynomial equation can be presented as follows:

$$Y = \beta_0 + \beta_1 x_1 + \beta_2 x_2 + \beta_3 x_3 + \beta_4 x_4 + \beta_{12} x_1 x_2 + \beta_{13} x_1 x_3 + \beta_{14} x_1 x_4 + \beta_{23} x_2 x_3 + \beta_{24} x_2 x_4 + \beta_{11} x_1^2 + \beta_{22} x_2^2 + \beta_{33} x_3^2 + \beta_{44} x_4^2 \quad (2)$$

**Table 1.** Process variables used in the central composite design (K = 4) with actual factor levels corresponding to coded factor levels.

| Variable | Variable code | Coded and actual levels | | | | |
|---|---|---|---|---|---|---|
| | | -2 | -1 | 0 | 1 | 2 |
| $AgNO_3$, 1 mM (%, v/v) | $X_1$ | 0.2 | 0.5 | 1 | 1.5 | 2 |
| Incubation period (h) | $X_2$ | 24 | 48 | 72 | 96 | 120 |
| Initial pH level | $X_3$ | 6 | 7 | 8 | 9 | 10 |
| Inoculum size (%, v/v) | $X_4$ | 1 | 2 | 4 | 6 | 8 |

The graphical representation of the model equation results in response surface plots that represent the individual and interactive effects of test variables on the response.

**Statistical Analysis**

The experimental data obtained were subjected to multiple linear regressions using Microsoft Excel 2007 to evaluate the analysis of variance (ANOVA). The quality of fit of the regression model was expressed *via* the correlation coefficient (R), the coefficient of determination ($R^2$), and the adjusted $R^2$, and its statistical significance was determined by an *F*-test. The optimal value of activity was estimated using the Solver function of Microsoft Excel tools. The statistical software package STATISTICA software (Ver. 8.0; StatSoft Inc., Tulsa, USA) was used to plot the three-dimensional surface plots, in order to illustrate the relationship between the responses and the experimental levels of each of the variables utilized in this study.

**Characterization of Silver Nanoparticles**

**UV–visible spectral analysis.** The biosynthesized silver nanoparticles using the cell-free supernatant were monitored by changes in color. AgNPs were characterized by a UV-vis spectrophotometer (Jenway UV/Visible- 2605 spectrophotometer, England) scanning in the range of 300–600 nm at regular intervals. Cell-free supernatant without addition of silver nitrate was used as a control throughout the experiment.

**Fourier-transform infrared spectroscopy analysis.** The interaction between protein and AgNPs was analyzed by Fourier transform-infrared spectroscopy (FTIR). The synthesized AgNPs sample was freeze dried and diluted with potassium bromide (in the ratio of 1:100) to make a pellet. The FTIR spectrum of samples was recorded on a FTIR instrument (FTIR-8400S). The measurement was carried out in the range of 500−4,000 $cm^{-1}$ at a resolution of 1 $cm^{-1}$.

**Antimicrobial activity of AgNPs by agar diffusion method.** Antimicrobial activity was tested for the biosynthesized AgNPs and cell-free supernatant against bacterial pathogens (obtained from Northern Regional Research Laboratory Peoria, Illinois 61604 USA) of gram-positive (*Staphylococcus aureus* NRRL B-313) and gram-negative bacteria (*Pseudomonas aeruginosa* NRRL B-23) and yeast (*Candida albicans* NRRL Y- 477) using the well-diffusion method on Luria-Bertani (LB) agar plates. A 100 µl bacterial

**Table 2.** Full factorial central composite design matrix of four process variables and mean response for biosynthesis of silver nanoparticles by *Streptomyces aegyptia* NEAE 102.

| Run | $AgNO_3$, 1 mM (%, v/v) | Incubation period (h) | Initial pH level | Inoculum size (%, v/v) | Absorbance at 400 nm | |
|---|---|---|---|---|---|---|
| | | | | | Experimental | Predicted |
| 1 | 0 | 2 | 0 | 0 | 1.246 | 1.400 |
| 2 | -2 | 0 | 0 | 0 | 0.124 | 0.143 |
| 3 | 0 | -2 | 0 | 0 | 0.011 | -0.062 |
| 4 | 2 | 0 | 0 | 0 | 0.135 | 0.197 |
| 5 | 0 | 0 | 2 | 0 | 2.5 | 2.562 |
| 6 | 0 | 0 | 0 | 0 | 0.101 | 0.101 |
| 7 | 0 | 0 | -2 | 0 | 1.103 | 1.121 |
| 8 | 0 | 0 | 0 | 0 | 0.101 | 0.101 |
| 9 | 0 | 0 | 0 | -2 | 1.097 | 1.087 |
| 10 | 0 | 0 | 0 | 2 | 0.154 | 0.245 |
| 11 | 1 | 1 | -1 | -1 | 0.886 | 0.884 |
| 12 | 1 | -1 | 1 | -1 | 0.226 | 0.462 |
| 13 | 1 | 1 | -1 | 1 | 0.411 | 0.363 |
| 14 | 1 | 1 | 1 | -1 | 2.5 | 2.251 |
| 15 | 0 | 0 | 0 | 0 | 0.101 | 0.101 |
| 16 | -1 | -1 | -1 | -1 | 0.584 | 0.525 |
| 17 | 1 | -1 | -1 | 1 | 0.466 | 0.472 |
| 18 | 0 | 0 | 0 | 0 | 0.101 | 0.101 |
| 19 | -1 | 1 | 1 | 1 | 1.707 | 1.640 |
| 20 | -1 | -1 | 1 | 1 | 0.401 | 0.426 |
| 21 | 1 | -1 | 1 | 1 | 0.345 | 0.150 |
| 22 | -1 | -1 | -1 | 1 | 0.207 | 0.352 |
| 23 | -1 | 1 | -1 | 1 | 0.237 | 0.024 |
| 24 | -1 | 1 | -1 | -1 | 0.464 | 0.554 |
| 25 | 1 | 1 | 1 | 1 | 1.499 | 1.582 |
| 26 | -1 | 1 | 1 | -1 | 2.3 | 2.317 |
| 27 | 0 | 0 | 0 | 0 | 0.101 | 0.101 |
| 28 | 0 | 0 | 0 | 0 | 0.101 | 0.101 |
| 29 | 1 | -1 | -1 | -1 | 0.674 | 0.637 |
| 30 | -1 | -1 | 1 | -1 | 0.803 | 0.747 |

suspension of each bacterial test organism was used to prepare bacterial lawns. Agar wells of 6 mm diameter were prepared with the help of a sterilized stainless-steel cork borer. The wells were loaded with 50 µl of AgNPs solution and 50 µl of cell-free supernatant without $AgNO_3$ as a control. The plates were incubated at 30°C for 24 h and then were examined for the presence of inhibition zones. The diameter of such zones of inhibition was measured and the mean value for each organism was recorded and expressed in millimeter unit.

## Results and Discussion

### Extracellular Biosynthesis of Silver Nanoparticles

The biosynthesis of silver nanoparticles was performed by using 100 ml of cell-free supernatant of *Streptomyces aegyptia* NEAE 102 treated with 1% (v/v) of 1 mM aqueous $AgNO_3$. The reaction mixture was kept in dark to avoid a photolytic reaction. Immediately, the pale yellow colored reaction mixture turned into a brown color within one minute indicating the formation of AgNPs (Fig. 1A). The biosynthesis of silver nanoparticles by *Streptomyces aegyptia* NEAE 102 was quite fast as in our previous work [4] and required far less time than previously published strains. The time required for completion of nanoparticle production varied from 24 to 120 h; this lengthy reaction is the one major drawback of biological synthesis and must be corrected if it is to compete with chemical procedures for

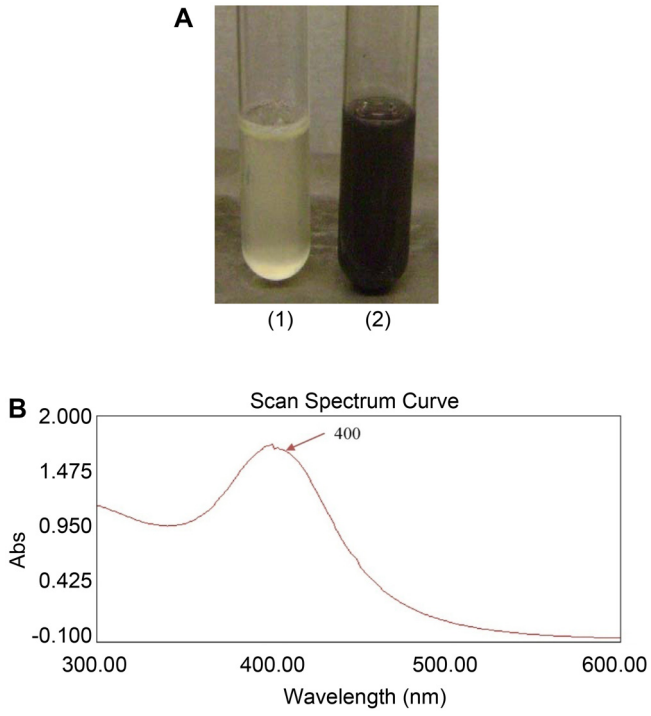


**Fig. 1.** Analyses of AgNPs produced by *Streptomyces aegyptia* NEAE 102.

(**A**) Visible observation of AgNPs biosynthesis by *Streptomyces aegyptia* NEAE 102: (1) Cell-free supernatant. (2) After exposure to $AgNO_3$ solution (1 mM). (**B**) UV–Vis absorption spectrum of silver nanoparticles synthesized by cell-free supernatant of *Streptomyces aegyptia* NEAE 102. The absorption spectrum of silver nanoparticles exhibited a strong broad peak at 400 nm, and observation of such a band is assigned to the surface plasmon resonance of the particles.

nanoparticle synthesis [29, 39].

### UV-Visible Spectral Analysis

In order to determine the formation of extracellular AgNPs, the reaction mixture was monitored by UV–Vis absorption spectrum scanning in the range of 300–600 nm. The specific surface plasmon resonance (SPR) spectra of silver nanoparticles produced by the *Streptomyces aegyptia* NEAE 102 revealed a strong absorption peak at 400 nm, indicating the presence of AgNPs (Fig. 1B). The position and shape of the plasmon absorption of silver nanoclusters strongly depend on particle size, stabilizing molecules, or surface adsorbed particles, as well as the dielectric constant of the medium [10]. According to Mie's theory [16], only a single SPR band is expected in the absorption spectra of spherical nanoparticles, whereas anisotropic particles could give rise to two or more SPR bands depending on the shape of the particles. The number of SPR peaks increases as the symmetry of the nanoparticle decreases [33]. Past studies suggested that DNA, sulfur-containing proteins [17], and NADH and its dependent enzymes are possibly involved in the biosynthesis of AgNPs by the bioreduction of silver ion to metallic silver [27]. Chun *et al.* [3] reported that NADH-dependent enzymes play a key role in these biosynthetic and biotransformation reactions as an electron carrier.

The UV–vis spectrum (Fig. 1B) clearly indicates the formation of AgNPs in the solution and the band corresponding to the surface plasmon resonance occurs at 400 nm. Ahmad *et al.* [1] showed that the band corresponding to the surface plasmon resonance occurs at 415 nm, and the exact position of absorbance depends on a number of factors such as the dielectric constant of the medium, size of the particle, *etc*.

### Optimization of Silver Nanoparticles Biosynthesis Using Response Surface Methodology

In order to evaluate the relationship between response and independent variables and to determine the maximum silver nanoparticles biosynthesis corresponding to the optimal levels of $AgNO_3$ concentration ($X_1$), incubation period ($X_2$), initial pH ($X_3$), and inoculum size ($X_4$), a second-order polynomial model was proposed to calculate the optimal levels of these variables. The results of experiments are represented in Table 2. The results showed considerable variation in the silver nanoparticles biosynthesis. Treatment runs 5, 14, and 26 showed a high silver nanoparticles biosynthesis (≥ 2.3). The maximum silver nanoparticles biosynthesis (2.5) was achieved in runs 5 and 14 under the conditions of 1 mM $AgNO_3$ (1–1.5% (v/v)), incubation period (72–96 h), initial pH (9–10), and inoculum size (2–4% (v/v)), whereas the minimum silver nanoparticles biosynthesis (0.011) was observed in run number 3.

By applying multiple regression analysis on experimental data of central composite design, a second-order polynomial model explains the role of each variable and their second-order interactions on silver nanoparticles biosynthesis. The determination coefficient ($R^2$) values provide a measure of how much variability in the observed response values can be explained by the experimental factors and their interactions. When $R^2$ is closer to 1, correlation is better between the experimental values and the values predicted by the second order polynomial model. The high $R^2$ value implies high degree of correlation between the observed and predicted values [20]. In this case, the value of the determination coefficient ($R^2$ = 0.98138) indicates that 98.138% of the variability in the response was attributed to the given independent variables, and only 1.862% of the total variations are not explained by the independent variables.

**Table 3.** Analysis of variance for optimization of silver nanoparticles biosynthesis using central composite design.

| | df | SS | MS | *F*-test | Significance *F* (*P*-value) |
|---|---|---|---|---|---|
| Regression | 14 | 15.7362 | 1.1240 | 56.4763 | 2.19E-10 |
| Residual | 15 | 0.2985 | 0.0199 | | |
| Total | 29 | 16.0348 | | | |

df, Degree of freedom; SS, Sum of squares; MS, Mean sum of squares; F, Fisherss function; Significance *F*, Corresponding level of significance.

In addition, the value of the adjusted determination coefficient (Adj. $R^2$ = 0.96401) was also very high, which indicates a high significance of the model. A higher value of the correlation coefficient (R = 0.99065) signifies an excellent correlation between the independent variables, which indicated a good correlation between the experimental and predicted values. Thus, the analysis of the response trend using the model was considered to be reasonable.

ANOVA was employed to test the significance and adequacy of the model. This was carried by Fisher's statistical test for the analysis of variance. The *F*-value indicates the influence (significance) of each controlled factor on the tested model; the results are presented in Table 3. The ANOVA of the regression model demonstrated that the model is highly significant, as was evident from the Fisher's *F*-test (56.4763) and a very low probability value (2.19E-10). The significance of each coefficient was determined by *t*-values and *P*-values, which are listed in Table 4. The *P*-values denote the significance of the coefficients and are also important in understanding the pattern of the mutual interactions between the variables. It can be seen from the degree of significance that the linear and quadratic effects of $X_2$ (incubation period), $X_3$ (initial pH), and $X_4$ (inoculum size) are significant, meaning that they can act as limiting factors and little variation in their value will alter the product production rate. Furthermore, the probability values of the coefficient suggest that among the four variables studied, $X_2$ (incubation period) and $X_3$ (initial pH) shows maximum interaction between the two variables (0.000), indicating that 100% of the model is affected by these variables, followed by interaction between $AgNO_3$ concentration($X_1$) and initial pH($X_3$). On the other hand, among the different interactions, the interaction between $X_1$ ($AgNO_3$ concentration), $X_2$ (incubation period); interaction between $X_1$ ($AgNO_3$ concentration), $X_4$ (inoculum size); interaction between $X_3$ (initial pH), $X_4$ (inoculum size); and linear and quadratic effects of $X_1$ did not show significant effect on silver nanoparticles biosynthesis. In order to evaluate the relationship between dependent and independent variables and to determine the maximum

**Table 4.** Estimated regression coefficients for optimization of silver nanoparticles biosynthesis using central composite design.

| Variables | Coefficients | Main effect | *t*-Stat | *P*-Value | Confidence level (%) |
|---|---|---|---|---|---|
| Intercept | 0.1010 | | 1.7537 | 0.0999 | 90.011 |
| $AgNO_3$ concentration ($X_1$) | 0.0136 | 0.027 | 0.4717 | 0.6439 | 35.607 |
| Incubation period ($X_2$) | 0.3653 | 0.731 | 12.6865 | 0.0000 | 100.000 |
| Initial pH level ($X_3$) | 0.3603 | 0.721 | 12.5100 | 0.0000 | 100.000 |
| Inoculum size ($X_4$) | -0.2104 | -0.421 | -7.3069 | 0.0000 | 100.000 |
| $X_1X_2$ | 0.0545 | 0.109 | 1.5453 | 0.1431 | 85.688 |
| $X_1X_3$ | -0.0991 | -0.198 | -2.8105 | 0.0132 | 98.682 |
| $X_1X_4$ | 0.0021 | 0.004 | 0.0603 | 0.9528 | 4.725 |
| $X_2X_3$ | 0.3853 | 0.771 | 10.9232 | 0.0000 | 100.000 |
| $X_2X_4$ | -0.0893 | -0.179 | -2.5306 | 0.0231 | 97.693 |
| $X_3X_4$ | -0.0369 | -0.074 | -1.0455 | 0.3123 | 68.767 |
| $X_1X_1$ | 0.0172 | 0.034 | 0.6396 | 0.5321 | 46.792 |
| $X_2X_2$ | 0.1420 | 0.284 | 5.2708 | 0.0001 | 99.991 |
| $X_3X_3$ | 0.4352 | 0.870 | 16.1572 | 0.0000 | 100.000 |
| $X_4X_4$ | 0.1412 | 0.282 | 5.2429 | 0.0001 | 99.990 |

*t*, Student's test; *P*, corresponding level of significance.

Multiple, R 0.99065; R Square, 0.98138; Adjusted R Square, 0.96401.

silver nanoparticles biosynthesis corresponding to the optimum levels of $AgNO_3$ concentration ($X_1$), incubation period ($X_2$), initial pH ($X_3$), and inoculum size ($X_4$), a second-order polynomial model (Eq. (3)) was proposed to calculate the optimum levels of these variables. By applying the multiple regression analysis on experimental data, the second-order polynomial equation that defines predicted response (Y) in terms of the independent variables ($X_1$, $X_2$, $X_3$, and $X_4$) was obtained:

$$Y_{(\text{Silver nanoparticles biosynthesis})} = 0.101 + 0.0136\ X_1 + 0.365\ X_2 + 0.360\ X_3 - 0.210\ X_4 + 0.055\ X_1 X_2 - 0.099\ X_1 X_3 + 0.002\ X_1 X_4 + 0.385\ X_2 X_3 - 0.089\ X_2 X_4 - 0.037\ X_3 X_4 + 0.0172\ X_1^2 + 0.142\ X_2^2 + 0.435\ X_3^2 + 0.141\ X_4^2 \quad (3)$$

where Y is the predicted response, $X_1$ the coded value of $AgNO_3$ concentration, $X_2$ the coded value of incubation period, $X_3$ the coded value of initial pH, and $X_4$ the coded value of inoculum size.

A comparison was made between the experimental and theoretical predictions by the model. The predicted and observed responses are presented in Table 2. This result shows that the predictive accuracy of the model is high.

The Pareto chart illustrates the order of significance of the variables affecting silver nanoparticles biosynthesis in the central composite design, as shown in Fig. 2. Among the four variables, the quadratic effect of initial pH showed the highest positive significance by 18.502%. Next to the quadratic effect of initial pH, the interaction between incubation period and initial pH showed a positive effect by 16.377%. The interaction between initial pH and inoculum size showed the higher negative effect by 1.568%.

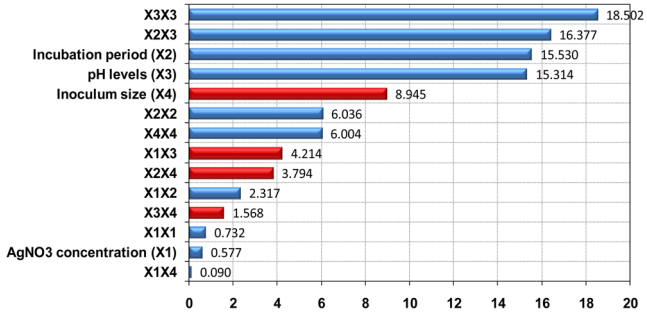


**Fig. 2.** Pareto chart illustrating the order of significance of the variables affecting the AgNPs biosynthesis by *Streptomyces aegyptia* NEAE 102 (the red color represents negative effects and the blue color represents positive effects; Ranks (%) values range from 0.090 to 18.502).

The interaction effects and optimal levels of the variables were determined by plotting the response surface curves (shown in Figs. 3A–3F) when one of the variables is fixed at optimum value and the other two are allowed to vary. Fig. 3A shows that there is gradual increasing of the silver nanoparticles biosynthesis with increasing the levels of $AgNO_3$ concentration. The maximum silver nanoparticles yield appeared at high levels of incubation time. Fig. 3B shows that higher levels of pH support high silver nanoparticles yield. On the other hand, lower and middle levels of $AgNO_3$ concentration support relatively high levels of silver nanoparticles yield.

Fig. 3C represents the interaction between $AgNO_3$ concentration and inoculum size. It showed that a low level of inoculum size supports high silver nanoparticles yield and further increase in the inoculum size led to a decrease in the silver nanoparticles biosynthesis. On the other hand, the maximum silver nanoparticles biosynthesis was clearly situated close to the central point of $AgNO_3$ concentrations. Fig. 3D represents the three-dimensional plot as a function of pH and incubation time on silver nanoparticles biosynthesis. It was observed that there is gradual increasing of the silver nanoparticles biosynthesis with increasing both pH and incubation time. The maximum silver nanoparticles yield appeared at high levels of both pH and incubation time. Fig. 3E depicts the interaction of incubation time and inoculum size. The plot reveals that the low level of inoculum size and high level of incubation time supported high silver nanoparticles yield. Fig. 3F represents the three-dimensional plot as a function of pH and inoculum size on silver nanoparticles biosynthesis. According to the plot, alkaline initial pH caused maximum silver nanoparticles biosynthesis at a low level of inoculum size. The biosynthesis was decreased remarkably as the pH decreased, whereas further increase in the inoculum size resulted in a gradual decrease in silver nanoparticles yield.

A low inoculum may require a longer time for microbial multiplication and substrate utilization to produce the desired product. On the other hand, a high inoculum would ensure rapid proliferation of the microbial biomass. Thus, a balance between the proliferating biomass and substrate utilization would yield maximum activity as recorded by Ramachandran *et al*. [23]. As the concentration of inoculum increases, it is followed by an increase in cell mass, and, after a certain period, metabolic waste interferes with the production of metabolites due to degradation of the product occurring. A lower inoculum density may reduce product formation, whereas a higher inoculum may lead to poor product formation, especially the large

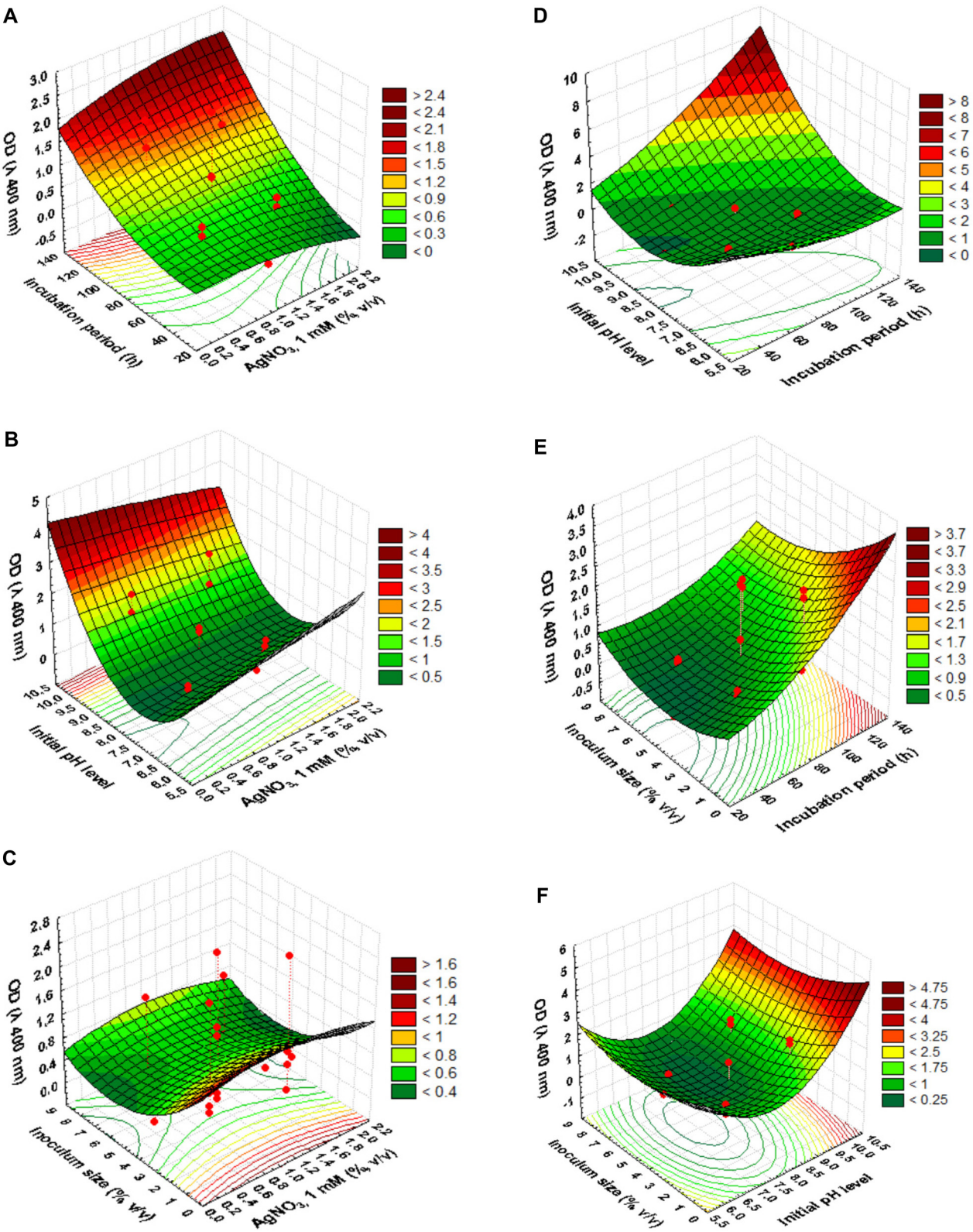


**Fig. 3.** Three-dimensional response surface (**A–F**) showing the interactive effects of independent variables ($AgNO_3$ 1 mM (%, v/v), incubation period (h), pH levels, inoculum size (%, v/v)) on biosynthesis of silver nanoparticles.

accumulation of toxic substances, and can also cause the reduction of dissolved oxygen and nutrient depletion in the culture media [22]. The pH value of the cultivation medium is very important for growth of the microorganism, characteristic of their metabolism, and hence for biosynthesis of metabolites. The hydrogen ion concentration may have a direct effect on the cell or it may indirectly affect it by varying the dissociation degree of the medium components [8].

**Verification of the Model**

Optimal concentrations of the factors, obtained from the optimization experiment, were verified experimentally and compared with the predicted data. The measured silver nanoparticles biosynthesis was 2.4 OD at 400 nm, where the predicted value from the polynomial model was 2.32 OD at 400 nm. The verification revealed a high degree of accuracy of the model of more than 96.6%, indicating the model validation under the tested conditions. The optimal levels of the process variables for silver nanoparticles biosynthesis by *Streptomyces aegyptia* NEAE 102 were 1 mM $AgNO_3$ (1.5% (v/v)), incubation period (96 h), initial pH (9), and inoculum size (2% (v/v)).

**Antimicrobial Activity of Synthesized AgNPs**

The antimicrobial activity of synthesized nanoparticles was assessed using gram-positive (*Staphylococcus aureus* NRRL B-313) and gram-negative (*Pseudomonas aeruginosa* NRRL B-23) bacterial strains and yeast (*Candida albicans* NRRL Y- 477) by the well-diffusion method (Fig. 4). A control (cell-free fermentation broth without $AgNO_3$ addition) was also maintained in each plate. It was noticed that the produced nanoparticles displayed antimicrobial activity against selected test microorganisms. The highest antimicrobial activity was observed against *Pseudomonas aeruginosa* NRRL B-23 (28 mm), followed by *Staphylococcus aureus* NRRL B-313 (25 mm) and *Candida albicans* NRRL Y- 477 (25 mm). The negative control (culture broth without $AgNO_3$) did not show any activity (Fig. 4), which further confirms the antibacterial activity of silver nanoparticles. These findings are in agreement with previous studies that examined the antimicrobial activity of AgNPs against *Staphylococcus aureus* [28].

Metallic silver in the form of AgNPs has been reported as a potential antimicrobial agent. The antibacterial potency of silver is directly proportional to the concentration of silver ions in the solution [12]. A number of possible mechanisms are proposed for the antibacterial activity of AgNPs. Silver ions have been known to bind with the

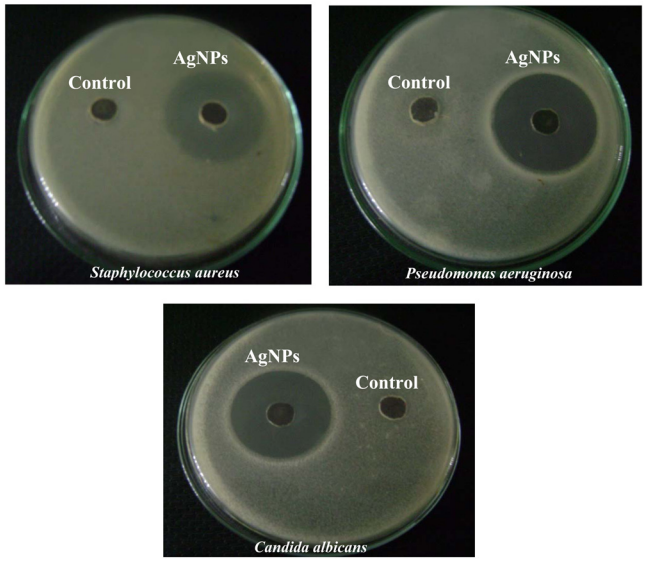


**Fig. 4.** Antibacterial activity of silver nanoparticles produced by *Streptomyces aegyptia* NEAE 102 against: gram-positive bacteria (*Staphylococcus aureus*), gram-negative bacteria (*Pseudomonas aeruginosa*), and yeast (*Candida albicans*).

negatively charged bacterial cell wall, resulting in the rupture and consequent denaturation of cellular proteins, which leads to cell death [13]. The synthesized AgNPs with smaller size can act drastically on the cell membrane and further interact with DNA and causes inhibition of DNA replication [17], causing depletion of intracellular ATP by rupture of the plasma membrane or by blocking respiration in association with oxygen and sulfhydryl (SH) groups on the cell wall to form R S S R bonds, thereby leading to cell death [11]. Matsumura *et al*. [15] proposed that silver ions interact with the thiol groups of some of the major enzymes and inactivate them. Silver nanoparticles cause damage by possibly interacting with sulfur and phosphorus-containing compounds such as DNA [32].

**Fourier Transform Infrared Analysis**

FTIR spectroscopy was used to characterize the surface chemistry of silver nanoparticles. The FTIR measurement can also be utilized to study the presence of a protein molecule in the solution. Fig. 5 shows the FTIR spectrum recorded from a pellet of potassium bromide and the silver nanoparticle produced by new isolate *Streptomyces aegyptia* NEAE 102 after 24 h of reaction. The spectrum showed the presence of six bands. The presence of bands at 1,056 and 1,616 $Cm^{-1}$ in the FTIR spectrum suggests the capping agent of biosynthesized nanoparticles possesses an aromatic

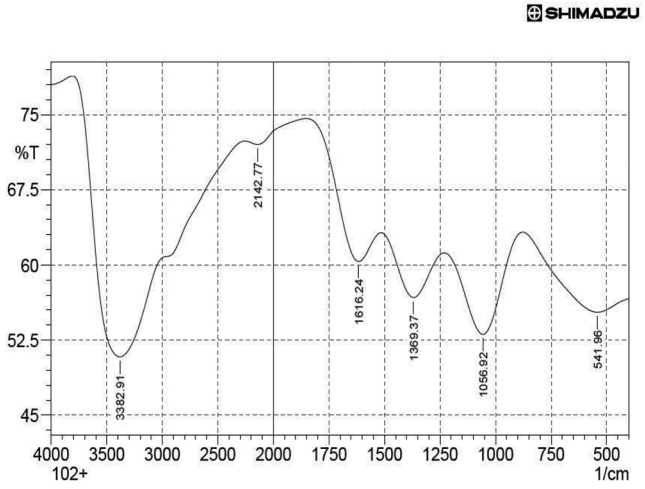


**Fig. 5.** FTIR spectrum recorded from a drop-coated film of silver nanoparticles synthesized by *Streptomyces aegyptia* NEAE 102.

amine group. In addition, the vibrations located at 1,369 and 2,142 $Cm^{-1}$ are attributed to the C-O stretching mode. Furthermore, the FTIR spectrum of biosynthesized silver nanoparticles also revealed a peak at 3,382 $Cm^{-1}$ of the stretching vibration of O-H bonds.

This type of FTIR spectrum supports the presence of a protein type of compound on the surface of biosynthesized nanoparticles, confirming that metabolically produced proteins act as capping agents during production and prevent the reduced silver particles agglomeration. In fact, the carbonyl groups from amino acid residues as well as peptides of proteins are known for their strong silver binding property. It has been suggested that the stability of the AgNPs generated using cell-free culture supernatants could be due to the presence of a proteinaceous capping agent that prevents aggregation of the nanoparticles [25].

**Energy-Dispersive X-Ray Spectroscopy**

Energy-dispersive X-ray spectroscopy (EDX) is an analytical technique used for the elemental analysis or chemical characterization of a sample. In the current study, for the confirmation of AgNPs, EDX spectroscopy analysis was performed, which confirmed the presence of elemental silver by the signals (Fig. 6). The optical absorption band peak in the range of 3 to 4 keV is typical for the absorption of metallic silver nanocrystallites [14]. However, there were other EDX peaks for Na, C, O, and Cl, suggesting that they were mixed precipitates from the centrifuged cell-free supernatant.

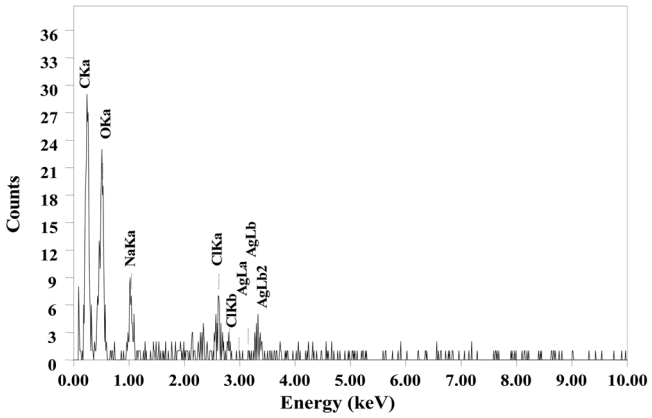


**Fig. 6.** EDX spectrum showing a peak between 3 and 4 keV, confirming the presence of silver.

In conclusion, this study revealed that the novel actinomycete *S. aegyptia* NEAE 102 synthesized silver nanoparticles extracellularly. The produced silver nanoparticles showed single surface plasmon resonance at 400 nm. The silver nanoparticles formed were characterized by UV–Vis spectroscopy and FTIR. This report presents data for the first time on the ability of the cell-free culture supernatant of *S. aegyptia* NEAE 102 to convert silver nitrate to AgNPs. The biosynthesized nanoparticles displayed a pronounced antimicrobial activity against gram-negative and gram-positive bacterial strains as well as yeast.

## References

1. Ahmad A, Mukherjee P, Senapati S, Mandal D, Khan MI, Kumar R, Sastry MJ. 2003. Extracellular biosynthesis of silver nanoparticles using the fungus *Fusarium oxysporum*. *Colloids Surf. B* **28:** 313-318.
2. Akaighe N, MacCuspie RI, Navarro DA, Aga DS, Banerjee S, Sohn M, Sharma VK. 2011. Humic acid-induced silver nanoparticle formation under environmentally relevant conditions. *Environ. Sci. Technol.* **45:** 3895-3901.
3. Chun YJ, Shimada T, Waterman MR, Guengerich FP. 2006. Understanding electron transport systems of *Streptomyces cytochrome* P450. *Biochem. Soc. Trans.* **34:** 1183-1185.
4. El-Naggar NE, Abdelwahed NAM. 2014. Application of statistical experimental design for optimization of silver nanoparticles biosynthesis by a nanofactory *Streptomyces viridochromogenes*. *J. Microbiol*. **52:** 53-63.
5. El-Naggar NE, Sherief AA, Hamza SS. 2001. *Streptomyces aegyptia* sp. nov., a novel cellulolytic streptomycete isolated from soil in Egypt. *Afr. J. Microbiol. Res.* **5:** 5308-5315.
6. Gao H, Liu M, Liu JT, Dai HQ, Zhou XL, Liu XY, *et al*. 2009.

Medium optimization for the production of avermectin B1a by *Streptomyces avermitilis* 14-12A using response surface methodology. *Bioresour. Technol.* **100:** 4012-4016.
7. Gurunathan S, Kalishwaralal K, Vaidyanathan R, Venkataraman D, Pandian SRK, Muniyandi J, *et al*. 2009. Biosynthesis, purification and characterization of silver nanoparticles using *Escherichia coli*. *Colloids Surf. B* **74:** 328-335.
8. Jain P, Pundir RK. 2011. Effect of fermentation medium, pH and temperature variation on antibacterial soil fungal metabolite production. *J. Agri. Technol*. **7:** 247-269.
9. Kowshik M, Ashtaputre S, Kharrazi S, Vogel W, Urban J, Kulkarni SK, Paknikar KM. 2003. Extracellular synthesis of silver nanoparticles by a silver-tolerant yeast strain MKY3. *Nanotechnology* **14:** 95-100.
10. Krishnaraj C, Jagan EG, Rajasekar S, Selvakumar P, Kalaichelvan PT, Mohan N. 2010. Synthesis of silver nanoparticles using *Acalypha indica* leaf extracts and its antibacterial activity against water borne pathogens. *Colloids Surf. B* **76:** 50-56.
11. Kumar VS, Nagaraja BM, Shashikala V, Padmasri AH, Madhavendra SS, Raju BD, Rao KSR. 2004. Highly efficient Ag/C catalyst prepared by electro-chemical deposition method in controlling microorganisms in water. *J. Mol. Catal. A Chem.* **223:** 313-319.
12. Lansdown AB. 2006. Silver in health care: antimicrobial effects and safety in use. *Curr. Probl. Dermatol.* **33:** 17-34.
13. Lin YE, Vidic RD, Stout JE, McCartney CA, Yu VL. 1998. Inactivation of *Mycobacterium avium* by copper and silver ions. *Water Res.* **32:** 1997-2000.
14. Magudapathy P, Gangopadhyay P, Panigrahi BK, Nair KGM, Dhara S. 2001. Electrical transport studies of Ag nanocrystallites embedded in glass matrix. *Physics B* **299:** 142-146.
15. Matsumura Y, Yoshikata K, Kunisaki S, Tsuchido T. 2003. Mode of bactericidal action of silver zeolite and its comparison with that of silver nitrate. *Appl. Environ. Microbiol.* **69:** 4278-4281.
16. Mie G. 1908. Beiträge zur Optik trüber Medien, speziell kolloidaler Metallösungen. *Ann. Phys.* **25:** 377-445.
17. Morones JR, Elechiguerra JL, Camacho A, Holt K, Kouri JB, Ramirez JT, Yacaman MJ. 2005. The bactericidal effect of silver nanoparticles. *Nanotechnology* **16:** 2346-2353.
18. Narayanan KB, Sakthivel N. 2010. Biological synthesis of metal nanoparticles by microbes. *Adv. Colloid Interface Sci.* **156:** 1-13.
19. Nelly YT, Kirkesali EI, Pataraya DT, Gurielidze MA, Kalabegishvili TL, Gvarjaladze DN, *et al*. 2011. Microbial synthesis of silver nanoparticles by *Streptomyces glaucus* and *Spirulina platensis*. *Nanomater. Appl. Properties* **2:** 306-310.
20. Panwal JH, Viruthagiri T, Baskar G. 2011. Statistical modeling and optimization of enzymatic milk fat splitting by soybean lecithin using response surface methodology. *Int. J. Nutr. Metab.* **3:** 50-57.
21. Peterson MSM, Bouwman J, Chen A, Deutsch M. 2007. Inorganic metallo-dielectric materials fabricated using two single-step methods based on the Tollen's process. *J. Colloid Interface Sci.* **306:** 41-49.
22. Rahman RNZA, Lee PG, Basri M, Salleh AB. 2005. Physical factors affecting the production of organic solvent-tolerant protease by *Pseudomonas aeruginosa* strain K. *Bioresour. Technol.* **96:** 429-436.
23. Ramachandran S, Patel AK, Nampoothiri KM, Francis F, Nagy V, Szakacs G, Pandey A. 2004. Coconut oil cake: a potential raw material for the production of α-amylase. *Bioresour. Technol.* **93:** 169-174.
24. Revankar MS, Lele SS. 2006. Increased production of extracellular laccase by the white rot fungus *Coriolus versicolor* MTCC 138. *World J. Microbiol. Biotechnol.* **22:** 921-926.
25. Saifuddin N, Wong CW, Nur Yasumira AA. 2009. Rapid biosynthesis of silver nanoparticles using culture supernatant of bacteria with microwave irradiation. *J. Chem.* **6:** 61-70.
26. Schultz S, Smith DR, Mock JJ, Schultz DA. 2000. Single target molecule detection with non-bleaching multicolor optical immunolabels. *Proc. Natl. Acad. Sci. USA* **97:** 996-1001.
27. Senapati S, Ahmad A, Khan MI, Sastry M, Kumar R. 2005. Extracellular biosynthesis of bimetallic Au-Ag alloy nanoparticles. *Small* **1:** 517-520.
28. Shahverdi AR, Fakhimi A, Shahverdi HR, Minaian S. 2007. Synthesis and effect of silver nanoparticles on the antibacterial activity of different antibiotics against *Staphylococcus aureus* and *Escherichia coli*. *Nanomed. Nanotech. Biol. Med.* **3:** 168-171.
29. Shankar SS, Rai A, Ahmad A, Sastry MJ. 2004. Rapid synthesis of Au, Ag and bimetallic Au shell nanoparticles using Neem. *J. Colloid Interf. Sci*. **275:** 496-502.
30. Shao K, Yao J. 2006. Preparation of silver nanoparticles *via* a non-template method. *Mater. Lett.* **60:** 3826-3829.
31. Shivaji S, Madhu S, Singh S. 2011. Extracellular synthesis of antibacterial silver nanoparticles using psychrophilic bacteria. *Process Biochem.* **46**: 1800-1807.
32. Singh M, Singh S, Prasad S, Gambhir IS. 2008. Nanotechnology in medicine and antibacterial effect of silver nanoparticles. *Dig. J. Nanomater. Biostruct.* **3:** 115-122.
33. Sosa IO, Noguez C, Barrera RG. 2003. Optical properties of metal nanoparticles with arbitrary shapes. *J. Phys. Chem.* **107:** 6269-6275.
34. Souza GIH, Marcato PD, Durán N, Esposito E. 2004. Utilization of *Fusarium oxysporum* in the biosynthesis of silver nanoparticles and its antibacterial activities. *In: IX National Meeting of Environmental Microbiology*. Curtiba, PR (Brazil).
35. Sun X, Luo Y. 2005. Preparation and size control of silver nanoparticles by a thermal method. *Mater. Lett.* **59:** 3847-3850.
36. Tang YX, Subramaniam VP, Lau TH, Lai YK, Gong DG, Kanhere PD, *et al*. 2011. *In situ* formation of large-scale Ag/

AgCl nanoparticles on layered titanate honey comb by gas phase reaction for visible light degradation of phenol solution. *Appl. Catal. B Environ*. **106:** 577-585.

37. Tomsic B, Simoncic B, Orel B, Zerjav M, Schroers HJ, Simoncic A, Samardzija Z. 2009. Antimicrobial activity of AgCl embedded in a silica matrix on cotton fabric. *Carbohydr. Polym.* **75:** 618-626.
38. Tsuji T, Iryo KN, Watanabe N, Tsuji M. 2002. Preparation of silver nanoparticles by laser ablation in solution: influence of laser wavelength on particle size. *Appl. Surf. Sci.* **202:** 80-85.
39. Vigneshwaran N, Arati Kathe N, Varadarajan PV, Rajan Nachane P, Balasubramanya RH. 2006. Biomimetics of silver nanoparticles by white rot fungus, *Phaenerochaete chrysosporium*. *Colloids Surf. B Interfaces* **53:** 55-59.
40. Wang XF, Li SF, Yua HG, Yu JG. 2011. *In situ* anion-exchange synthesis and photocatalytic activity of Ag8W4O16/AgCl-nanoparticle core–shell nanorods. *J. Mol. Catal. A Chem.* **334:** 52-59.